APC Mutation marks an aggressive subtype of *BRAF* mutant colorectal cancers

Short Title: WNT, *APC* mutation and Serrated Colorectal Cancer

Lochlan J. Fennell[1,2], Alexandra Kane[1,2,3], Cheng Liu[1,2,4], Diane McKeone[1], Winnie Fernando[1], Chang Su[1,2], Catherine Bond[1], Saara Jamieson[1], Troy Dumenil[1], Ann-Marie Patch[1], Stephen H. Kazakoff[1], John V. Pearson[1], Nicola Waddell[1,2], Barbara Leggett[1,2,5] and Vicki Whitehall[1,2,3]

[1]QIMR Berghofer Medical Research Institute, Queensland, Australia; [2]The University of Queensland, Australia; [3]Conjoint Internal Medicine Laboratory, Chemical Pathology, Pathology Queensland, Australia; [4]Envoi Specialist Pathologists, Queensland, Australia; [5]The Royal Brisbane and Women's Hospital, Queensland, Australia

Grant Support: This work was supported through funding from the National Health and Medical Research Council (Grant #: 1050455, 1063105), the Cancer Council Queensland (1160923), the RBWH Research Foundation and Pathology Queensland. VW is the recipient of a Senior Research Fellowship from the Gastroenterological Society of Australia. LF was supported by a Research Training Program Living Scholarship from the Australia Government, a Top-Up award from QIMR Berghofer and Australian Rotary Health. NW is funded by a National Health and Medical Research Council fellowship (Grant #: APP1139071).

Correspondence: Lochlan Fennell

Lochlan.Fennell@qimrberghofer.edu.au

Level 7 Clive Berghofer Cancer Research Centre,

QIMR Berghofer Medical Research Institute

300 Herston Rd, Herston, 4006

Australia

Disclosures: The authors declare no conflicts of interest.

Preprint: Fennell et al 2020, BioRxiv (ID: BIORXIV/2020/942904)

Synopsis:

We have comprehensively evaluated the somatic mutation landscape of WNT signaling regulators in serrated colorectal cancers. We identified a mosaic of mutations that may be responsible for elevating WNT signaling in this context. Approximately 20% of serrated colorectal cancers harbor truncating *APC* mutation, and these cancers confer extremely poor prognoses.

Keywords: *BRAF*; Colorectal Cancer; Serrated Neoplasia; WNT signaling; *APC* Mutation; Cancer Genomics

Abstract

Background & Aims: WNT activation is a hallmark of colorectal cancer. *BRAF* mutation is present in 15% of colorectal cancers, and the role of mutations in WNT signaling regulators in this context is unclear. Here we evaluate the mutational landscape of WNT signaling regulators in *BRAF* mutant cancers.

Methods: We performed exome-sequencing on 24 *BRAF* mutant colorectal cancers and analysed these data in combination with 175 publicly available *BRAF* mutant colorectal cancer exomes. We assessed the somatic mutational landscape of WNT signaling regulators, and performed hotspot and driver mutation analyses to identify potential drivers of WNT signaling. The effects of *Apc* and *Braf* mutation were modelled, *in vivo*, using the $Apc^{min/+}$ and $Braf^{V637}$/*Villin-*$Cre^{ERT2/+}$ *mouse,* respectively.

Results: *RNF43* was the most frequently mutated WNT signaling regulator (41%). Mutations in the beta-catenin destruction complex occurred in 48% of cancers. Hotspot analyses identified potential cancer driver genes in the WNT signaling cascade, including *MEN1*, *GNG12* and *WNT16*. Truncating *APC* mutation was identified in 20.8% of cancers. Truncating *APC* mutation was associated with early age at diagnosis ($P< 2x10^{-5}$), advanced stage (P<0.01), and poor survival (P=0.026). $Apc^{min/+}$/$Braf^{V637}$ animals had more numerous and larger SI and colonic lesions (P<0.0001 and P<0.05, respectively), and a markedly reduced survival (Median survival: 3.2 months, $P=8.8x10^{-21}$) compared to animals with *Apc* or *Braf* mutation alone.

Conclusions:

The WNT signaling axis is frequently mutated in *BRAF* mutant colorectal cancers. *WNT16* and *MEN1* may be novel drivers of aberrant WNT signaling in colorectal cancer. Co-mutation of *BRAF and APC* generates an extremely aggressive neoplastic phenotype that is associated with poor patient outcome.

Background

Colorectal cancer is a heterogeneous disease that arises through two main molecular pathways. The conventional pathway, which accounts for 75-80% of all colorectal cancer diagnoses, is initiated by biallelic inactivation of *APC* and progresses to cancer via mutations in *KRAS* and alterations to the *TP53* gene. By contrast, the serrated neoplasia pathway is initiated by activating mutations in *BRAF* and often progresses to malignancy via MLH1 hypermethylation, microsatellite instability and a plethora of epigenetic alterations. At the transition to dysplasia, serrated lesions usually acquire mutations that increase WNT signaling. Sessile serrated lesions (SSLs) acquire missense *APC* mutations[1], and truncating *RNF43* mutations[2]. In traditional serrated adenomas (TSAs), common WNT pathway aberrations include *RSPO3* fusions [3,4], mutations of *CTNNB1*[3] and mutation of *APC*[3].

In the normal enterocytes the WNT signaling cascade exists to support stemness, differentiation and development. Appropriate levels of WNT signal are maintained intracellularly by the *β*-catenin destruction complex. The complex consists of AXIN, APC, GSK3*β*, and CK1α. The destruction complex ubiquitinates *β-catenin* in the cytosol, triggering its subsequent proteasomal degradation. In the absence of the destruction complex, β-catenin translocates to the nucleus, forms a complex with the TCF/LEF molecules and p300 to activate the expression of genes supporting the stem phenotype. Constitutive WNT signaling is deleterious to the cell and thus in the absence of exogenous stimuli the β-catenin destruction complex patrols the cytosol and degrades β-catenin. WNT signaling is activated by the binding of extracellular WNT ligands to frizzled receptors residing on the cell surface. This triggers the sequestering of the destruction complex to the cell membrane and facilitates the build-up of β-catenin, which enters the nucleus and activates WNT target genes.

Approximately 45-50% of *BRAF* mutant cancers show dysregulated WNT signaling[1], and thus the WNT signaling pathway appears important to serrated colorectal neoplasia. In conventional colorectal carcinogenesis, WNT signaling is dysregulated via truncating mutations of *APC* and loss of 5q21, the region where the *APC* gene resides[5]. This dysregulation occurs very early in the evolution of conventional adenomas. However numerous studies have indicated that mutation of *BRAF* is almost never identified in such *APC* mutated adenomas even when they develop advanced histological features [6,7]. This suggests that *BRAF* and *APC* mutations are mutually exclusive in conventional adenomas.

In the serrated neoplastic pathway where the initiating mutation is *BRAF,* WNT signaling only commonly becomes dysregulated when the benign polyp transitions to malignancy. Truncating *RNF43* mutations may alter WNT signaling, but these are predominantly present in mismatch repair deficient *BRAF* mutant cancers[2,8], and there is controversy as to whether *RNF43* mutation affects canonical WNT signaling[9]. Epigenetic silencing of WNT pathway members is another possible mechanism for altering canonical WNT pathway activity. Methylation of *SFRP* genes increases WNT signaling[10] and is common in colorectal cancer[11]. Similarly DNA methylation induced inactivation of *DKK* genes, which are antagonists of WNT signaling, occurs in ~20% of all colon cancers[12]. The frequency of WNT signaling dysregulation being due to *APC* mutation is not well established.

Here we have conducted a large-scale genomic analysis of the somatic mutations that underlie WNT signaling activation in *BRAF* mutant colorectal cancer. We hypothesise that WNT

signaling activation in *BRAF* mutant cancers will be heterogeneous, and a mosaic of alterations underpin WNT signaling to achieve a “just-right” level of pathway activation.

Methods

Cohorts included in the study

We assessed the somatic mutational landscape of 199 *BRAF* mutant cancers from four distinct sources. This included cancers from The Cancer Genome Atlas project (n=51)[7,13], the Dana Faber Cancer Institute (Giannakis et al 2016, n=111)[14], the Clinical Proteomic Tumor Analysis Consortium (Suhas et al 2019, n=13)[15] and additional *BRAF* mutant cancers that were sequenced as part of this study (methods detailed below, n=24). For analyses involving the *APC* tumour suppressor gene we included additional targeted sequenced data from the Memorial Sloan-Kettering Cancer Centre (Yaeger et al 2018, n=76)[16]. This dataset was limited to a panel of genes and as such was excluded from other analyses. Supplementary Figure 1 shows similar tumor mutation burden across each cohort. Clinicopathological details of samples included in this study and mutational data are available as supplementary materials (Supplementary Table S1 and S2).

DNA extraction, library preparation and exome sequencing of local samples

Cancer and germline samples were obtained from patients at the Royal Brisbane and Women's Hospital, Brisbane, Australia at the time of surgery. All participants gave their written, informed consent prior to participating in the study and the study was approved by the QIMR Berghofer Human Research Ethics Committee (P460, P773). DNA was isolated from whole blood using the salt precipitation method as previously reported[17]. Cancer samples were snap-frozen in liquid nitrogen and DNA extracted using the AllPrep DNA/RNA/Protein mini kit (QIAGEN, Germany) as previously reported [18]. Exome-sequencing libraries were generated using the Agilent SureSelect Human All Exon V4+UTR capture platform (Agilent, CA, USA). Libraries were sequenced to a target depth of 200-fold coverage on a 100 bp paired-end sequencing run using an Illumina HiSeq 2000 instrument. Sequence reads were trimmed using Cutadapt (v1.9) [19] and aligned to the GRCh37 reference with BWA-MEM (v0.7.12) [20]. Alignments were duplicate-marked with Picard (v1.129, https://broadinstitute.github.io/picard/) and coordinate-sorted using Samtools (v1.1) [21]. Single nucleotide substitution variants were detected using a dual calling strategy using qSNP (v2.0) [22] and the GATK HaplotypeCaller (v3.3-0) [23]. The HaplotypeCaller was also used to call short indels of ≤50 bp. Initial read filtering for all variants detected included: a minimum of 35 alignment matches in the CIGAR string, 3 or fewer mismatches in the MD field, and a mapping quality greater than 10. High confidence variants were selected with: a minimum coverage of 8 reads in the control data and 12 reads in the tumour data; at least 5 variant supporting reads present where the variant was not within the first or last 5 bases; at least 4 of the 5 reads with unique start positions; the variant was identified in reads of both sequencing directions; the variant was not less than 5 base pairs from a mono-nucleotide run of 7 or more bases in length. Variants were annotated with gene feature information and transcript or protein consequences using SnpEff (v4.0e) [24].

Assessing the somatic mutational landscape of WNT regulators

To assess the somatic mutational landscape of WNT signaling regulators we downloaded mutational annotation files for each cohort from the Genome Data Commons (TCGA,), cBioPortal (CPTAC), from supplementary materials (DFCI) or analysis of the Royal Brisbane and Women's Hospital, Brisbane cases. MAF files concatenated to form a combined MAF file comprised of 924,366 entries relating to 1411 samples. *BRAF* V600E mutant samples were subset from the larger dataset, yielding a total of 320,431 variants from 199 samples. As we

sought to investigator WNT, we further selected only genes that were members of the REACTOME signaling by WNT geneset (n=327 genes). The final dataset was comprised of 5,327 nonsynonymous variants in WNT signaling loci that corresponded to 199 samples.

Analysis of variants was performed using the MAFtools R package[25]. Cancer drivers were predicted using two orthogonal approaches (OncodriveClust[26]: Default parameters; OncodriveFML[27]: Scores: CADD v1.3, Signature: Computed by sample, remaining parameters: default). Driver mutation analyses were performed on the entire set of variants to accurately model the background mutational processes. Results from Non-WNT loci were discarded and FDR corrections were performed on the remaining P values that pertain to tests performed on genes in the WNT signaling pathway. Somatic interactions (co-mutations and mutual exclusivity) were identified by performing fishers exact test on pairs of genes.

Murine model of Apc and Braf mutation

To model the effects of *Apc* and *Braf* mutation on colorectal neoplasia we utilized two murine models. The *Apc*$^{Min/+}$ mouse has a mono-allelic mutation at codon 851 and recapitulates human germline *APC* mutation. In both humans and mice, progression is governed by the loss of the remaining allele. Our second model, the *Braf*$^{CA/CA}$/Villin-Cre$^{ERT2/+}$ mouse [28,29], is an inducible model of *Braf* mutant colorectal neoplasia. Recombination of the mutant *Braf* V637E allele is induced at 2 weeks of age by a single intraperitoneal injection of tamoxifen (75mg/kg). The *Braf* V637E allele is the murine analogue of the *BRAF* V600E human mutation. To model the effects of *Apc* mutation and *Braf* mutation we crossed *Apc*$^{Min/+}$ mice with *Braf*$^{CA/CA}$/Villin-Cre$^{ERT2/+}$. Animals were monitored biweekly for signs of distressed and humanely euthanized when such signs were identified, as per our approved protocol (QIMR Berghofer Animal Ethics Committee; P1208). For survival analysis, animals were deemed to be deceased if they were euthanized due to distress. If animals reached the prescribed endpoints of the experiment without any signs of distress they were deemed to have survived and were censored for survival analysis.

At sacrifice the gastrointestinal tract from oesophagus to rectum was removed, cleaned and opened longitudinally. Macroscopic lesions were bisected to obtain both molecular and histological data. Matched normal hyperplastic tissue was taken minimum five centimetres from the site of the lesion. Histological assessment of lesions and lesion counts was performed on haematoxylin and eosin stained sections from formalin-fixed, paraffin-embedded blocks by specialist gastrointestinal anatomical pathologists.

Sanger Sequencing

Sanger sequencing was performed to assess the G7 repeat track of *WNT16*. PCR conditions were as follows: 1X GoBuffer (ProMega, USA), 2.5mM $MgCl_2$, 0.25mM dNTP, 0.25uM Forward Primer (5' GGCAACATGACAGAGTGTTCC 3'), 0.25uM Reverse Primer (5' GCCATACTGGACATCATCGG 3'), 0.25uM Syto9, 1U GoTaq DNA polymerase (ProMega, USA), 50ng DNA; Cycing: 95□C hold for two minutes, 40X cycles of 95□C for 30 seconds, 60□C for 30 seconds, 72□C for 45 seconds, followed by a 72□C hold for five minutes at the end of cycle 40. Sequencing was performed as per Fennell et al[30].

Statistical Analysis

All statistical analysis was performed in Microsoft Open R (v3.5.1). Students T-Tests were performed for hypothesis testing of continuous variables. Logistic regression analyses were

employed to examine the probability of mutations over patient age. The likelihood-ratio test was performed to assess associations with categorical variables and fishers exact test to examine for mutual exclusivity of mutations in gene-pairs.

Results

The somatic mutation landscape of WNT signaling in BRAF mutated cancers

To assess the degree of variation in genetic alterations of WNT signaling pathway genes, we collated whole exome-sequencing data of *BRAF* mutant colorectal cancers from three previously published studies [7,14,15], combined with 24 samples that were sequenced in-house (total n=199). We limited WXS variants to genes in the WNT signaling cascade, as identified in the REACTOME signaling by WNT gene set (n=327 genes). The mean number of WNT pathway mutations per sample was 16.7±13.6, and was highly correlated with overall tumour mutation burden ($P= 4.08x10^{-85}$, $r^2=0.86$). *RNF43* was the most commonly mutated gene (41%, Figure 1). 35.3% of samples had a truncating mutation in *RNF43*. *KMT2D*, *TRRAP,* and *APC* were mutated in 33%, 30% and 28% of samples, respectively (Figure 1).

The *β-catenin* destruction complex is an important regulator of canonical WNT signaling. It is comprised of *APC, AXIN1, AXIN2,* and GSK3*β* (Figure 2). We next evaluated how frequently mutations occur in any component of this complex or in CTNNB1 itself. 48% of all cancers had mutations in at least one of these five genes. Mutations in *APC* and *AXIN2*, but not *AXIN1*, are significantly mutually exclusive (P<0.05). Missense mutations in *CTNNB1* have been reported to render the molecule impervious to ubiquitin-mediated destruction. *CTNNB1* mutations occur in 9% of samples. Missense *CTNNB1* mutations were mutually exclusive with truncating *APC* mutations.

Somatic mutation interaction analysis identifies co-mutated WNT signaling loci and mutual exclusivity of truncating APC and RNF43 mutations

We performed somatic mutation interaction analyses to examine for mutations in genes that are mutually exclusive and those that tend to co-occur. We found evidence for co-occurring mutations in 222 gene pairs (Figure 3). Table 1 summarizes the top 20 pairs of genes, which have co-occurring mutations. As truncating mutations are more likely to influence the final protein, we next examined somatic interactions between truncating mutations in WNT pathway genes (Figure 3). We identified statistical evidence for somatic interactions between 75 gene pairs. 96% were between co-mutated gene pairs (Supplementary Table S3, Table 1). Truncating *APC* mutation was mutually exclusive to truncating mutations in both *RNF43* (P0.0003, OR:0.20), and ZNRF3 (P=0.001, OR: 0). *AMER1* truncating mutations were mutually exclusive to *RNF43* mutation (P=0.043, OR:0.12).

Mutation clustering analysis reveals mutational hotspots in nine WNT signaling genes

We next sought to identify driver genes using the OncodriveCLUST algorithm. This method identifies potential driver genes using a positional clustering method and operates on the assumption that clusters of mutations, or “mutational hotspots” are more likely to occur in oncogenes. In keeping with previous studies [2,8,30,31(p43)], *RNF43* was identified as a putative cancer driver (P=0.07). Somatic mutations in *MEN1*, a gene identified as a familial cancer risk gene and as an inducer of genome wide hypermethylation, were identified as putative drivers. *MEN1* was mutated in 4% (8/199, P<0.001) of samples, and most of the identified mutations were frameshift deletions at R521. Moreover, *WNT16* was implicated as a potential cancer driver (P=0.06). *WNT16* harbours a mutational hotspot at G165. This codon resides in a G7 repeat track that was the subject of frameshift indels in 15 cancers (Table 2). We used Sanger sequencing to orthogonally validate the presence of *WNT16* hotspot mutations in *BRAF* mutant

cancers (n=79) and identified frameshift mutations in 20.2% (16/79) of cancers (Supplementary Figure S2).

We used oncodriveFML, an orthogonal computational method of predicting cancer drivers based on predictions of functionality, to identify other potential driver genes that do not necessarily harbour clusters of mutations. This analysis identified 11 potential cancers drivers in the WNT signaling cascade, three of which were identified by oncodriveCLUST (*RNF43*: P=7.22x10^{-6}, *MEN1*: P= 0.02, and *GNG12*: P=0.012). Other genes that were identified include members of the beta-catenin destruction complex (*APC:* P=7.22x10^{-6}*, AXIN1:* P<0.01*, AXIN2: P=0.0001*), *ZNRF3 (*P=7.22x10^{-6}), *SOX9 (*P=7.22x10^{-6}), *BCL9L* (P<0.001), *PYGO2* (P<0.001), and *WNT11* (P=0.045).

Co-mutation of APC and BRAF represents a unique and aggressive subtype of BRAF mutant cancers

We next evaluated the relationship between *BRAF* mutation and *APC* mutation in further detail to characterize the clinical and molecular correlates of this subtype of cancers. We supplemented the 199 *BRAF* mutant exomes assessed earlier in the manuscript with 76 *BRAF* mutant cancers that were subjected to targeted sequencing as part of Yaeger et al 2018[16]. Truncating mutation was present in 20% of *BRAF* mutant cancers. We examined whether there was a relationship between age at diagnosis and *APC* mutation by logistic regression analysis. The probability of truncating *APC* mutation occurring in a *BRAF* mutant cancer decreases markedly with age from ~60% in patients diagnosed at age 40, to <10% of patients diagnosed at >90 years of age (Logistic Regression P=3.74x10^{-7}). The average age of patients with a *BRAF*^{V600E}/*APC*$^{\text{Truncated}}$ cancer was significantly lower than both patients with a *BRAF* $^{\text{V600E}}$/*APC*$^{\text{Missense}}$ tumour (61 vs 72, P=2.03x10^{-5}, Table 3) and a patient with a *BRAF* $^{\text{V600E}}$/*APC*$^{\text{Wild-type}}$ cancer (61 vs 71, P=9.3x10^{-6}). *BRAF*^{V600E}/*APC*$^{\text{Truncated}}$ cancers were more likely to be left sided when compared with *BRAF*^{V600E}/*APC*^{Missense} cancer (24.5% vs 4.2%, P=0.02, Table 3). There was no difference in frequency of CIMP versus either missense or wild-type APC cancers. 42.3% of *BRAF*^{V600E}/*APC*$^{\text{Truncated}}$ cancers were microsatellite unstable. MSI is less frequent than both *BRAF* $^{\text{V600E}}$/*APC*$^{\text{Missense}}$ (91.3%, P=5.3x10^{-5}, Table 3) and *BRAF* $^{\text{V600E}}$/*APC*$^{\text{Wild-type}}$ (53.8%, P=0.14) cancers.

BRAF^{V600E}/*APC*$^{\text{Truncated}}$ cancers were aggressive cancers, with 67.3% of patients presenting with metastatic disease. In contrast, only 36.4% and 45.7% of *BRAF* $^{\text{V600E}}$/*APC*$^{\text{Missense}}$ and *BRAF* $^{\text{V600E}}$/*APC*$^{\text{Wild-type}}$ cancers presented at stage III/IV (P= 0.01 and 0.002 versus *BRAF*^{V600E}/*APC*$^{\text{Truncated}}$, respectively). *BRAF*^{V600E}/*APC*$^{\text{Truncated}}$ cancers that were also microsatellite stable were enriched further for late-stage disease, with 100% of these patients presenting with metastatic disease (Stage III or IV), and 88% with distant metastases (Stage IV).

Furthermore, univariable analysis of survival indicated that *BRAF*^{V600E}/*APC*$^{\text{Truncated}}$ cancers have a significantly poorer median survival (504 days vs 1390 days, Log-rank P=0.026, n=32 and n=78 for truncating mutant and wild-type, respectively; Figure 4A). The five-year survival of *BRAF*^{V600E}/*APC*$^{\text{Truncated}}$ patients was 12%. By contrast the five year survival of *BRAF*^{V600E}/*APC*$^{\text{Wild-Type}}$ patients was 42%. We performed multivariate survival analysis, including age at diagnoses, gender, stage and microsatellite instability as potential prognosticators. Using the cox-proportional hazard method, microsatellite instability status, and gender are significantly independently associated with survival. Truncating *APC* mutation trends toward conferring

independent negative prognostic implications, however this failed to reach the threshold for significance (Table 4, P=0.17). Collectively these data indicate that activating mutation of *BRAF* and truncating mutation of *APC* represent an aggressive subtype of colorectal cancers that occur at a relatively young age in comparison to *BRAF* mutant cancers more generally.

Mutation of Braf in APC$^{min/+}$ mouse results in massive polyp load, rapid disease progression and poor survival

To determine if we could recapitulate the apparently aggressive phenotype of co-mutation of *BRAF* and *APC* we crossed inducible *Braf^{V637}* mutant mice with *Apc$^{min/+}$* mice. The *Braf* mutation was induced at wean in *Apc$^{Min/+}$* mice and we compared the number of lesions per animal and survival to mice with just the mutant *Braf* allele or the mutant *Apc* allele.

We next assessed differences in survival between *Apc$^{Min/+}$ (n=29), Braf^{V637}(n=15), and APC$^{Min/+}$/ Braf^{V637}* mice (n=22). Animals were regarded as having survived and were censored if they were healthy at the time of sacrifice, animals regarded as deceased if the animal had to be euthanized due to illness. 100% of *Braf* mutant animals survived to 12 months, as did 81.25% of *Apc* mutant animals. Mutation of both *Braf* and *Apc* significantly reduced the survival of the animals (P= 8.8×10^{-21}, Figure 4B). The median survival of animals with both *Apc* and *Braf* mutation was 3.2 months. No animal with both mutations survived longer than six months.

We assessed polyp load by microscopic enumeration. Animals with *Braf* and *Apc* mutations alone develop an average of 4.6 and 16.55 polyps in the small intestine, respectively. Animals with both *Braf* and *Apc* mutation simultaneously develop significantly more lesions in the SI (*P<0.0001,* Figure 5A*)*. Animals with *Braf* or *Apc* mutation rarely developed colonic or caecal lesions (mean lesions per mouse: 0.11 and 1.1, respectively, Figure 5B). In contrast, dual mutation of *Apc* and *Braf* resulted in the accumulation of an average of 59.82 colonic/caecal lesions per animal (P<0.0001, Figure 5B). We did not observe a significant increase in lesion size in the small intestine between groups, however we did observe significantly larger lesions in the colon and caecum of animals bearing both *Apc* and *Braf* mutation (P<0.0001, Figure 5C). Lesions had a morphology that was reminiscent of human conventional adenomas, rather than dysplastic serrated lesions.

Discussion

Here we have investigated the role of somatic mutation in shaping the WNT signaling landscape of colorectal cancers bearing the *BRAF* mutation. We have shown that 48% of *BRAF* mutant cancers mutate at least one member of the B-catenin destruction complex. Other common modes of activation including mutation of *RNF43* and *ZNRF3*. We have identified a number of novel mutations that may alter the WNT signaling landscape of cancers. These include *MEN1*, a known WNT pathway tumour suppressor, and *WNT16*, a WNT ligand that may act as an antagonist of ligand mediated WNT activation. Both *MEN1* and *WNT16* harbour hotspot frameshift mutations that were identified as potential drivers by computational analysis. Mutation of *RNF43* was mutually exclusive to mutation of *APC*. We examined the clinical and molecular correlates of *BRAF* mutant cancers bearing truncating mutations of *APC,* which occurred in 20% of samples. These cancers were predominantly microsatellite stable, and late stage. Cancers with a truncating *APC* mutation occurred at an average age that was >10 years lower than the wider cohort of *BRAF* mutant cancers. Survival analysis revealed a significantly poorer prognosis for this subtype of patients. Using murine models of *Apc* and *Braf* mutation, we show that mutating both genes results in an extensive phenotype with massive lesion burden. Animals had a median survival of 3.2 months, and no animal bearing both mutations survived longer than 6 months. Collectively these data indicate that mutation of both *BRAF* and *APC* results in an aggressive and rapidly progressing cancer phenotype and confers a poor prognosis.

WNT signaling underpins colorectal carcinogenesis. In the conventional pathway WNT signaling is usually activated via bi-allelic inactivation of the APC tumour suppressor gene at the beginning of the tumourigenic process. However, the mechanisms governing WNT pathway activation in the serrated neoplasia pathway, which is uniquely marked by *BRAF* mutation, is less clear. In the present study, we sought to identify WNT signaling genes that are mutated in the context of *BRAF* mutant serrated colorectal neoplasia. We obtained exome sequencing data from 175 *BRAF* mutant colorectal cancers from four previously published studies[7,14,15,32] and sequenced a further 24 *BRAF* mutant samples collected locally. Our analyses revealed a mosaic of mutations in WNT signaling regulators, including well-known WNT regulators such as *RNF43, APC, AXIN2 and ZNRF3.* Our analysis identified significant mutual exclusivity between truncating mutations of *RNF43* and *APC.* Likewise, ZNRF3 mutation was mutually exclusive to truncating mutations of *APC*. This association was present only when missense mutations were not included. It is possible that the addition of a truncating *APC* mutation in this context is disadvantageous to tumour progression. Therefore, mutation of *RNF43/ZNRF3* may create a genetic dependency on *APC*. If true, exploiting the dependency on *APC,* a canonical tumour suppressor gene, may be a novel therapeutic treatment for patients with an *RNF43* mutated cancer.

We next examined the exome sequencing data to identify potential novel drivers of WNT signaling activation in colorectal cancer. We adopted a mutational clustering based approach to identify potential cancer drivers based on the presence of mutational hotspots, as implemented in the oncodriveCLUST algorithm[26]. Reassuringly, *RNF43*, which has two mutational hotspots[2,8,30] was successfully identified as a cancer driver. *RSPO* fusions, which have been implicated in WNT dysregulation of serrated lesions and cancers[4,33], were not identified due to technological limitations. It is likely that some cancers in this cohort harboured such fusions given the frequency of RSPO fusions previously reported. We identified eleven other potential cancer driver genes in the WNT signaling cascade. *MEN1* was mutated in eight samples and

most mutations were frameshift alterations at codon R521. Germline *MEN1* mutations result in multiple endocrine neoplasia type 1, a tumour predisposition syndrome. It has also been identified as a tumour suppressor gene in a number of different cancer types, including tumours of the parathyroid[34(p1)], entero-pancreatic neuroendocrine cancers[35(p1)], and carcinoids[36]. Interestingly, especially in the context of highly methylated *BRAF* mutant cancers, loss of *MEN1* has been associated with aberrant DNMT1 activity and an altered DNA methylation landscape. To our knowledge, *MEN1* alterations have not been previously reported in colorectal cancer, nor is colorectal cancer a typical presentation of *MEN1* syndrome. It is possible these patients had an underlying germline mutation in *MEN1,* and the mutations identified in this studied were the second hit at the locus.

WNT16 was also identified as a potential cancer driver gene. WNT16 is a WNT ligand, a seemingly unlikely candidate tumour suppressor. However, Nalesso et al [37] showed that while WNT16 was capable of binding Fzd receptors and activating canonical WNT signaling, the degree of activation was significantly lower when compared with the more abundant WNT3A. TOPFlash assays showed that costimulation with both WNT3A and WNT16 resulted in significantly less canonical WNT activation when compared with stimulation using WNT3A alone[37]. Thus, it appears WNT16 acts as a competitive inhibitor of Fzd and acts to ensure the homeostasis of WNT signaling. In cancer, loss of WNT16 may facilitate excessive canonical WNT activation by failure to compete with more potent WNT ligands, such as WNT3A and WNT8. As such, it is likely that WNT16 acts as a tumour suppressor. Inhibitors of WNT ligand secretion, such as porcupine inhibitors, are currently being trialed in colorectal and other solid tumours[38]. Cancers that lack WNT16 are prone to excessive ligand-dependent WNT activation[37(p16)] and may represent a subset of patients that could benefit from this therapy. Indeed, as much of *WNT16* mutations occur on a background of *RNF43* alterations, which has been shown to confer sensitivity to porcupine inhibitors[31], mutation of both genes could further sensitize cells to this class of drugs. Both functional and biomarker studies are required to determine whether WNT16 has a role in determining sensitivity to WNT-ligand inhibitors.

We recently assessed a series of 80 *BRAF* mutant cancers[1] and identified truncating *APC* mutation in 11% of these cancers. It has been postulated that truncating APC mutation is uncommon in the context of pre-existing BRAF mutation because the dysregulation of WNT signal is too profound in this cellular context. This is consistent with the model proposed by Albuquerque et al [39] and indicates that mutations such as *RNF43*/*ZNRF3* provides a “just-right” level of WNT signaling to confer a selective advantage. However, the present study has confirmed that a minority of *BRAF* mutant cancers do carry a truncating APC mutation. The higher proportion of cancers bearing both *APC* and *BRAF* mutation in the present study may be due to selection bias in the present series with a higher proportion of late stage microsatellite stable cancer included.

APC mutations were much more common in minority of *BRAF* mutant cancers diagnosed at a younger age. The average age of *BRAF* mutant cancers harbouring *APC* mutation was 12 years less than *APC* wild-type. These cancers were more likely to be microsatellite stable, and present with metastatic disease. The median survival of patients with *BRAF* mutation and *APC* mutation was 64% lower than patients with *BRAF* mutation alone, and patients with both mutations had a five-year survival rate of 12%. These cancers appear to be highly aggressive and occur earlier in life. We generated a murine model to recapitulate mutation of *APC* and *BRAF* to examine interactions between these mutations and the consequences of mutating both

genes on polyp development and overall survival. We observed massive polyp loads in animals bearing both mutations, and a markedly reduced survival. 100% and 81.25% of *Braf* mutant and *Apc* mutant animals survived to 12 months. When we mutated both genes, no animals survived past six months and the median survival was reduced to a mere 3.2 months. While animals did not develop invasive cancer, and instead died due to polyp load, these data indicate that comutation of *APC* and *BRAF* in an enterocyte induces rapid neoplastic alterations and an overt proliferative phenotype. Collectively these data provide strong evidence that mutation of both *APC* and *BRAF,* whilst uncommon in humans, generates a remarkably aggressive neoplastic phenotype.

It is difficult to resolve how these particular cancers have evolved. Both *APC* and *BRAF* mutations are tumour-initiating events [28,40,41] and give rise to different precursor lesions[42]. Moreover, the cell of origin for *APC* initiated polyps and *BRAF* initiated polyps is hypothesized to differ. *APC* initiated lesions adhere to the "top-down" model[43], whereas *BRAF* mutant lesions are initiated in the stem compartment[44]. Methylation profiling of *BRAF* mutant and *APC* mutant cancers confirmed this model, and showed that *BRAF* mutant cancers had a methylation profile reminiscent of the intestinal stem cell[44(p)]. In our study, we observed no difference in the frequency of CIMP between *BRAF* mutants with *APC* mutation and those without, suggesting that these dual-mutant cancers may have arisen in the stem component, and therefore may have been initiated by *BRAF* and acquired an *APC* mutation at a later stage. However it is difficult to reconcile this with the rarity to which *APC* is mutated in *BRAF* mutant precursor lesions[1]. It is possible that, upon acquiring an *APC* mutation, progression to cancer is rapid and as a result identifying lesions in a transitional state is rare. This fits with the aggressive phenotype of these cancers. An alternative hypothesis, supported an age at diagnosis that is similar to conventional pathway cancers[18] and the morphology of our murine adenomas, is that polyps are initiated by *APC,* acquire a *BRAF* mutation. If this is the case such lesions must progress extremely rapidly to cancer as they are very rarely identified in large series of conventional adenomas.

In conclusion, here we have conducted a comprehensive survey of the somatic mutational landscape shaping WNT signaling in *BRAF* mutant serrated colorectal neoplasia. The mutational landscape of WNT signaling regulators is a mosaic that is underpinned by mutations in key driver genes, such as *RNF43* and *APC*. Mutations of *RNF43* and *APC* are mutually exclusive. We identified potential cancer driver genes in the WNT signaling axis. *MEN1* has previously been implicated in cancers of endocrine origin, but has not been identified as a tumour suppressor gene in colorectal cancer. We have identified a hotspot mutation in *MEN1* that effects 4% of *BRAF* mutant cancers. We have identified WNT16 as a potential driver gene by mutational hotspot analysis. WNT16 is a competitive inhibitor of canonical WNT and mutation of WNT16 is common in *BRAF* mutant cancers. Loss of WNT16 may increase the sensitivity of cancers to WNT ligand dependent canonical WNT signaling and thus WNT16 mutant cancers may be susceptible to inhibitors of WNT ligand secretion (ie. PORCN inhibitors). *BRAF* mutant colorectal cancers with truncating *APC* mutation tended to arise earlier in life, and presented at a significantly later stage. These cancers are extremely aggressive and survival of patients with both *BRAF* and *APC* mutation is poor (12% 5-year survival). *In vivo* modelling of *Apc* and *Braf* mutation revealed a dramatically increased tumour burden with the median survival of 3.2 months for animals with both mutations. Therefore, we conclude that co-mutation of *BRAF* and *APC* in colorectal cancers is conducive to an aggressive phenotype.

Table 1: Somatic interaction analysis identifies significantly co-occurring mutations in 222 gene pairs. Analysis of truncating mutations only identified 75 somatic interactions. The twenty most significant interactions are detailed in this table. For the remaining interactions, see Supplementary Table S3. P Values were calculated using the fishers exact test.

All Mutations					Truncating Mutations				
Gene 1	Gene 2	P Value	OR	Event	Gene 1	Gene 2	P Value	OR	Event
TRRAP	ITPR2	6.09E-06	6.011045	Co-Occurrence	TNRC6B	CHD8	0.000105	17.11726	Co-Occurrence
KMT2D	CREBBP	1.34E-05	4.366674	Co-Occurrence	APC	RNF43	0.000384	0.202421	Mutual Exclusivity
BCL9	ITPR3	0.00014	5.099699	Co-Occurrence	SMARCA4	GNG12	0.00064	43.38263	Co-Occurrence
WNT16	TNRC6C	0.000165	6.912418	Co-Occurrence	SOX7	WNT1	0.001325	32.98824	Co-Occurrence
WNT16	KMT2D	0.000178	5.325269	Co-Occurrence	APC	ZNRF3	0.001333	0	Mutual Exclusivity
ITPR2	BCL9L	0.000275	4.558515	Co-Occurrence	PPP3CA	BCL9L	0.003294	14.90311	Co-Occurrence
DVL2	CREBBP	0.000298	5.12913	Co-Occurrence	FZD3	CHD8	0.004894	16.65752	Co-Occurrence
CHD8	CLTC	0.000305	5.748636	Co-Occurrence	PYGO2	KMT2D	0.005244	10.39723	Co-Occurrence
ROR2	CREBBP	0.000315	4.665817	Co-Occurrence	SMARCA4	RNF43	0.00652	~	Co-Occurrence
CCDC88C	SCRIB	0.000374	6.740312	Co-Occurrence	TNRC6B	NLK	0.006741	16.41138	Co-Occurrence
CREBBP	TLE1	0.000454	6.384479	Co-Occurrence	SOX9	WNT11	0.006741	16.41138	Co-Occurrence
SOX9	AP2A2	0.000458	7.282798	Co-Occurrence	USP8	PPP2R5A	0.007373	33.08956	Co-Occurrence
DVL2	AMER1	0.000485	5.748333	Co-Occurrence	ITPR2	BCL9L	0.007892	6.481383	Co-Occurrence
DVL2	LRP5	0.000485	5.748333	Co-Occurrence	SOX13	ITPR3	0.008157	29.57061	Co-Occurrence
SOX7	AGO2	0.000499	7.121906	Co-Occurrence	TRRAP	TCF7L2	0.009844	11.15266	Co-Occurrence
SMARCA4	PSME4	0.000564	6.329348	Co-Occurrence	WNT16	KMT2D	0.011438	3.935969	Co-Occurrence
TLE4	BCL9L	0.00073	5.675492	Co-Occurrence	SOX13	FZD3	0.012072	22.44601	Co-Occurrence
CLTC	AMER1	0.000805	5.807688	Co-Occurrence	WNT1	FZD3	0.012072	22.44601	Co-Occurrence
BCL9	TCF7L2	0.000878	4.77049	Co-Occurrence	HECW1	GNG12	0.012072	22.44601	Co-Occurrence
ZNRF3	RNF43	0.000911	3.451942	Co-Occurrence	WNT1	GNG12	0.012072	22.44601	Co-Occurrence

Table 2: Position-based mutational analysis identifies nine potential cancer driver genes in the WNT signaling cascade.

Gene	Mutated Samples (n)	Positional Clusters	Mutations in Clusters	Cluster Score	P Value
MEN1	8	2	8	1	0.0007
GNG12	7	1	6	0.857142857	0.006
WNT16	25	2	18	0.668284271	0.06
RNF43	82	6	66	0.640721112	0.07

Table 3: Clinical and molecular characteristics of *BRAF* mutant cancers with *APC* mutation

			APC			P-value[1]		
		n	Truncating Mutation	Missense Mutation	Wild-Type	Truncating vs Missense	Truncating vs Wild-type	Missense vs Wild-type
Mean Age		273	60.8	72.4	70.6	**2.03×10^{-5}**	**9.3×10^{-6}**	0.34
Sex	Male	87 (31.8%)	18 (32%)	6 (24%)	63 (33%)	0.48	0.86	0.36
	Female	187 (68.2%)	39 (68%)	19 (76%)	129 (67%)			
Tumour Side	Left	42 (16.6%)	13 (25%)	1 (4%)	28 (16%)	**0.02**	0.16	0.08
	Right	211 (83.4%)	40 (75%)	23 (86%)	148 (84%)			
Stage	I	32 (12.9%)	3 (6%)	2 (9%)	27 (16%)	**0.01**	**0.002**	0.32
	II	93 (37.7%)	14 (27%)	12 (55%)	67 (39%)			
	III	59 (23.9%)	10 (19%)	6 (27%)	43 (25%)			
	IV	63 (25.5%)	25 (48%)	2 (9%)	36 (21%)			
CIMP	High	128 (81.0%)	20 (83%)	18 (95%)	90 (78%)	0.23	0.57	0.05
	Negative	30 (19.0%)	4 (17%)	1 (5%)	25 (22%)			
MSI	MSI	136 (54.8%)	22 (42%)	21 (91%)	93 (54%)	**5.3×10^{-5}**	0.14	**0.0002**
	MSS	112 (45.2%)	30 (58%)	2 (9%)	80 (46%)			

[1]P-values were obtained using the likelihood-ratio test for categorical variables, and the student's t-test for continuous variables. All statistical analyses were two-tailed

Table 4: Cox-proportional Hazard analysis of survival of *BRAF* mutant cancers.

Variable	Risk Ratio	95% CI	P Value
Microsatellite Instability (MSS)	2.41	1.18-4.95	0.016
Gender (Female)	1.93	1.04-3.57	0.0373
APC (Truncating)	1.63	0.80-3.32	0.1744
Stage (III/IV)	1.56	0.66-3.69	0.3083
Age (<50)	1.2	0.53-2.71	0.6545

References

1. Borowsky J, Dumenil T, Bettington M, et al. The role of APC in WNT pathway activation in serrated neoplasia. *Mod Pathol Off J U S Can Acad Pathol Inc*. 2018;31(3):495-504. doi:10.1038/modpathol.2017.150

2. Bond CE, McKeone DM, Kalimutho M, et al. RNF43 and ZNRF3 are commonly altered in serrated pathway colorectal tumorigenesis. *Oncotarget*. 2016;7(43):70589-70600. doi:10.18632/oncotarget.12130

3. Hashimoto T, Ogawa R, Yoshida H, et al. Acquisition of WNT Pathway Gene Alterations Coincides With the Transition From Precursor Polyps to Traditional Serrated Adenomas. *Am J Surg Pathol*. 2019;43(1):132-139. doi:10.1097/PAS.0000000000001149

4. Sekine S, Yamashita S, Tanabe T, et al. Frequent PTPRK-RSPO3 fusions and RNF43 mutations in colorectal traditional serrated adenoma. *J Pathol*. 2016;239(2):133-138. doi:10.1002/path.4709

5. Rowan AJ, Lamlum H, Ilyas M, et al. APC mutations in sporadic colorectal tumors: A mutational “hotspot” and interdependence of the “two hits.” *Proc Natl Acad Sci*. 2000;97(7):3352-3357. doi:10.1073/pnas.97.7.3352

6. Kambara T, Matsubara N, Nagao A, et al. Mtations in BRAF, KRAS, and APC, and CpG island methylation: Alternative pathways to colorectal cancer. *Cancer Res*. 2006;66(8 Supplement):81-81.

7. The Cancer Genome Atlas Network. Comprehensive molecular characterization of human colon and rectal cancer. *Nature*. 2012;487(7407):330-337. doi:10.1038/nature11252

8. Giannakis M, Hodis E, Jasmine Mu X, et al. RNF43 is frequently mutated in colorectal and endometrial cancers. *Nat Genet*. 2014;46(12):1264-1266. doi:10.1038/ng.3127

9. Tu J, Park S, Yu W, et al. The most common RNF43 mutant G659Vfs*41 is fully functional in inhibiting Wnt signaling and unlikely to play a role in tumorigenesis. *Sci Rep*. 2019;9(1):1-12. doi:10.1038/s41598-019-54931-3

10. Suzuki H, Watkins DN, Jair K-W, et al. Epigenetic inactivation of SFRP genes allows constitutive WNT signaling in colorectal cancer. *Nat Genet*. 2004;36(4):417-422. doi:10.1038/ng1330

11. Suzuki H, Gabrielson E, Chen W, et al. A genomic screen for genes upregulated by demethylation and histone deacetylase inhibition in human colorectal cancer. *Nat Genet*. 2002;31(2):141-149. doi:10.1038/ng892

12. Aguilera O, Fraga MF, Ballestar E, et al. Epigenetic inactivation of the Wnt antagonist DICKKOPF-1 (DKK-1) gene in human colorectal cancer. *Oncogene*. 2006;25(29):4116-4121. doi:10.1038/sj.onc.1209439

13. Y L, Ns S, T H, et al. Comparative Molecular Analysis of Gastrointestinal Adenocarcinomas. Cancer cell. doi:10.1016/j.ccell.2018.03.010

14. Giannakis M, Mu XJ, Shukla SA, et al. Genomic Correlates of Immune-Cell Infiltrates in Colorectal Carcinoma. *Cell Rep*. 2016;15(4):857-865. doi:10.1016/j.celrep.2016.03.075

15. Vasaikar S, Huang C, Wang X, et al. Proteogenomic Analysis of Human Colon Cancer Reveals New Therapeutic Opportunities. *Cell*. 2019;177(4):1035-1049.e19. doi:10.1016/j.cell.2019.03.030

16. R Y, Wk C, Md L, et al. Clinical Sequencing Defines the Genomic Landscape of Metastatic Colorectal Cancer. Cancer cell. doi:10.1016/j.ccell.2017.12.004

17. Miller SA, Dykes DD, Polesky HF. A simple salting out procedure for extracting DNA from human nucleated cells. *Nucleic Acids Res*. 1988;16(3):1215.

18. Fennell L, Dumenil T, Wockner L, et al. Integrative Genome-Scale DNA Methylation Analysis of a Large and Unselected Cohort Reveals Five Distinct Subtypes of Colorectal Adenocarcinomas. *Cell Mol Gastroenterol Hepatol*. April 2019. doi:10.1016/j.jcmgh.2019.04.002

19. Martin M. Cutadapt removes adapter sequences from high-throughput sequencing reads. *EMBnet.journal*. 2011;17(1):10-12. doi:10.14806/ej.17.1.200

20. Li H. Aligning sequence reads, clone sequences and assembly contigs with BWA-MEM. *ArXiv13033997 Q-Bio*. May 2013. http://arxiv.org/abs/1303.3997. Accessed February 6, 2020.

21. Li H, Handsaker B, Wysoker A, et al. The Sequence Alignment/Map format and SAMtools. *Bioinforma Oxf Engl*. 2009;25(16):2078-2079. doi:10.1093/bioinformatics/btp352

22. Kassahn KS, Holmes O, Nones K, et al. Somatic Point Mutation Calling in Low Cellularity Tumors. *PLOS ONE*. 2013;8(11):e74380. doi:10.1371/journal.pone.0074380

23. McKenna A, Hanna M, Banks E, et al. The Genome Analysis Toolkit: A MapReduce framework for analyzing next-generation DNA sequencing data. *Genome Res*. 2010;20(9):1297-1303. doi:10.1101/gr.107524.110

24. Cingolani P, Platts A, Wang LL, et al. A program for annotating and predicting the effects of single nucleotide polymorphisms, SnpEff: SNPs in the genome of Drosophila melanogaster strain w1118; iso-2; iso-3. *Fly (Austin)*. 2012;6(2):80-92. doi:10.4161/fly.19695

25. Mayakonda A, Lin D-C, Assenov Y, Plass C, Koeffler HP. Maftools: efficient and comprehensive analysis of somatic variants in cancer. *Genome Res*. 2018;28(11):1747-1756. doi:10.1101/gr.239244.118

26. D T, A G-P, N L-B. OncodriveCLUST: Exploiting the Positional Clustering of Somatic Mutations to Identify Cancer Genes. Bioinformatics (Oxford, England). doi:10.1093/bioinformatics/btt395

27. Mularoni L, Sabarinathan R, Deu-Pons J, Gonzalez-Perez A, López-Bigas N. OncodriveFML: a general framework to identify coding and non-coding regions with cancer driver mutations. *Genome Biol*. 2016;17(1):128. doi:10.1186/s13059-016-0994-0

28. Bond CE, Liu C, Kawamata F, et al. Oncogenic BRAF mutation induces DNA methylation changes in a murine model for human serrated colorectal neoplasia. *Epigenetics*. 2018;13(1):40-48. doi:10.1080/15592294.2017.1411446

29. Kane AM, Fennell LJ, Liu C, et al. Alterations in signaling pathways that accompany spontaneous transition to malignancy in a mouse model of BRAF mutant microsatellite stable colorectal cancer. *Neoplasia*. 2020;22(2):120-128. doi:10.1016/j.neo.2019.12.002

30. Fennell LJ, Clendenning M, McKeone DM, et al. RNF43 is mutated less frequently in Lynch Syndrome compared with sporadic microsatellite unstable colorectal cancers. *Fam Cancer*. 2018;17(1):63-69. doi:10.1007/s10689-017-0003-0

31. X J, Hx H, Jd G, et al. Inactivating Mutations of RNF43 Confer Wnt Dependency in Pancreatic Ductal Adenocarcinoma. Proceedings of the National Academy of Sciences of the United States of America. doi:10.1073/pnas.1307218110

32. S S, Ew S, S D, et al. Recurrent R-spondin Fusions in Colon Cancer. Nature. doi:10.1038/nature11282

33. Sekine S, Ogawa R, Hashimoto T, et al. Comprehensive characterization of RSPO fusions in colorectal traditional serrated adenomas. *Histopathology*. 2017;71(4):601-609. doi:10.1111/his.13265

34. Z Y, C SC, M S, et al. Loss of MEN1 Activates DNMT1 Implicating DNA Hypermethylation as a Driver of MEN1 Tumorigenesis. Oncotarget. doi:10.18632/oncotarget.7279

35. Agarwal SK. The future: genetics advances in MEN1 therapeutic approaches and management strategies. *Endocr Relat Cancer*. 2017;24(10):T119-T134. doi:10.1530/ERC-17-0199

36. Marini F, Falchetti A, Luzi E, Tonelli F, Maria Luisa B. Multiple Endocrine Neoplasia Type 1 (MEN1) Syndrome. In: Riegert-Johnson DL, Boardman LA, Hefferon T, Roberts M, eds. *Cancer Syndromes*. Bethesda (MD): National Center for Biotechnology Information (US); 2009. http://www.ncbi.nlm.nih.gov/books/NBK7029/. Accessed January 20, 2020.

37. Nalesso G, Thomas BL, Sherwood JC, et al. WNT16 antagonises excessive canonical WNT activation and protects cartilage in osteoarthritis. *Ann Rheum Dis*. 2017;76(1):218-226. doi:10.1136/annrheumdis-2015-208577

38. Rodon J, Argilés G, Connolly RM, et al. Abstract CT175: Biomarker analyses from a phase I study of WNT974, a first-in-class Porcupine inhibitor, in patients (pts) with advanced solid tumors. *Cancer Res*. 2018;78(13 Supplement):CT175-CT175. doi:10.1158/1538-7445.AM2018-CT175

39. Albuquerque C, Breukel C, van der Luijt R, et al. The 'just-right' signaling model: APC somatic mutations are selected based on a specific level of activation of the β-catenin signaling cascade. *Hum Mol Genet*. 2002;11(13):1549-1560. doi:10.1093/hmg/11.13.1549

40. Fearon ER, Vogelstein B. A genetic model for colorectal tumorigenesis. *Cell*. 1990;61(5):759-767. doi:10.1016/0092-8674(90)90186-I

41. Rad R, Cadiñanos J, Rad L, et al. A Genetic Progression Model of BrafV600E-Induced Intestinal Tumorigenesis Reveals Targets for Therapeutic Intervention. *Cancer Cell*. 2013;24(1):15-29. doi:10.1016/j.ccr.2013.05.014

42. Rk P, M B, A S, C R. An Update on the Morphology and Molecular Pathology of Serrated Colorectal Polyps and Associated Carcinomas. Modern pathology□: an official journal of the United States and Canadian Academy of Pathology, Inc. doi:10.1038/s41379-019-0280-2

43. Shih I-M, Wang T-L, Traverso G, et al. Top-down morphogenesis of colorectal tumors. *Proc Natl Acad Sci U S A*. 2001;98(5):2640-2645. doi:10.1073/pnas.051629398

44. Bormann F, Rodríguez-Paredes M, Lasitschka F, et al. Cell-of-Origin DNA Methylation Signatures Are Maintained during Colorectal Carcinogenesis. *Cell Rep*. 2018;23(11):3407-3418. doi:10.1016/j.celrep.2018.05.045

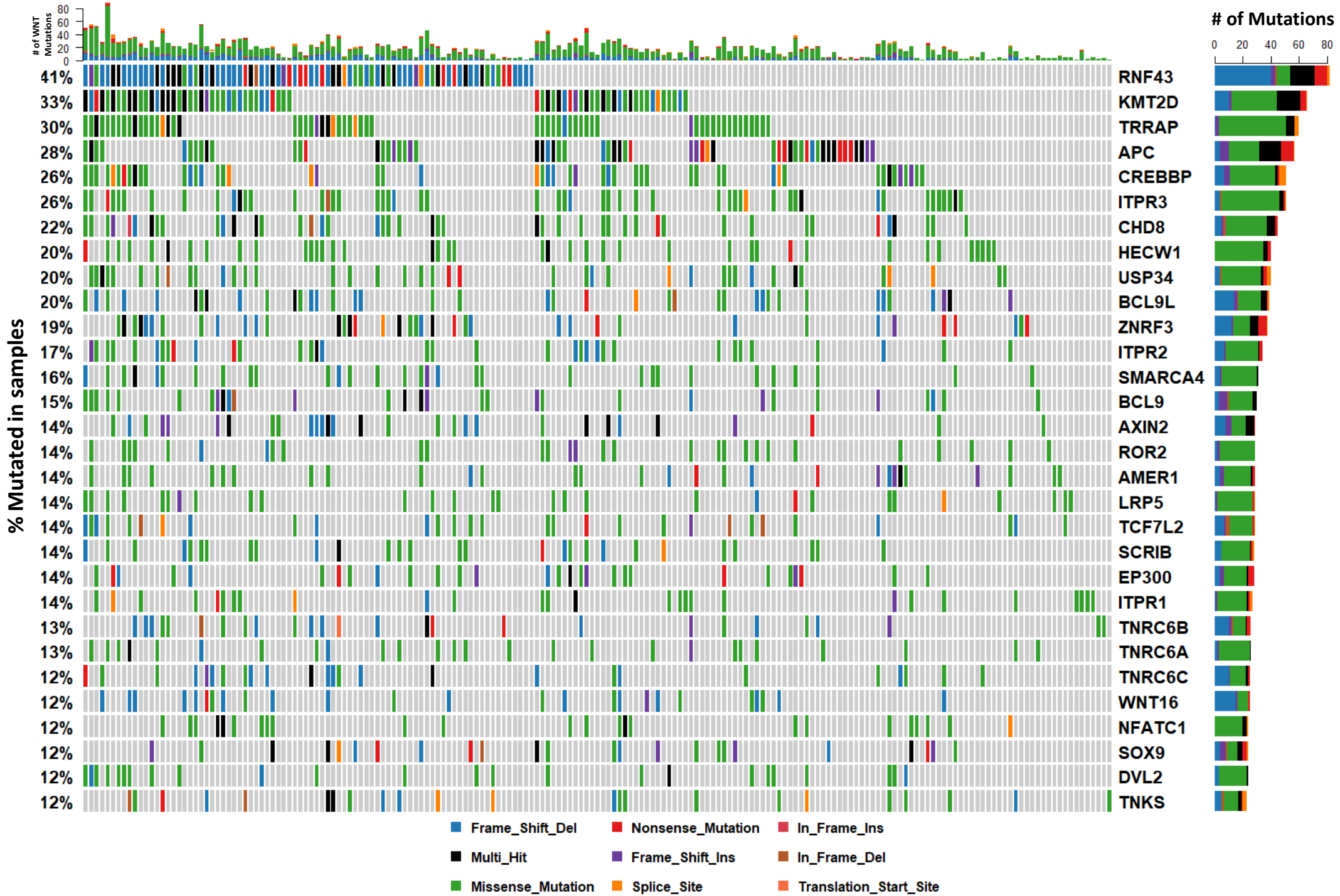
# of WNT Mutations
80
60
40
20
0
# of Mutations
0
20
40
60
80
% Mutated in samples
41% RNF43
33% KMT2D
30% TRRAP
28% APC
26% CREBBP
26% ITPR3
22% CHD8
20% HECW1
20% USP34
20% BCL9L
19% ZNRF3
17% ITPR2
16% SMARCA4
15% BCL9
14% AXIN2
14% ROR2
14% AMER1
14% LRP5
14% TCF7L2
14% SCRIB
14% EP300
14% ITPR1
13% TNRC6B
13% TNRC6A
12% TNRC6C
12% WNT16
12% NFATC1
12% SOX9
12% DVL2
12% TNKS
Frame_Shift_Del
Nonsense_Mutation
In_Frame_Ins
Multi_Hit
Frame_Shift_Ins
In_Frame_Del
Missense_Mutation
Splice_Site
Translation_Start_Site

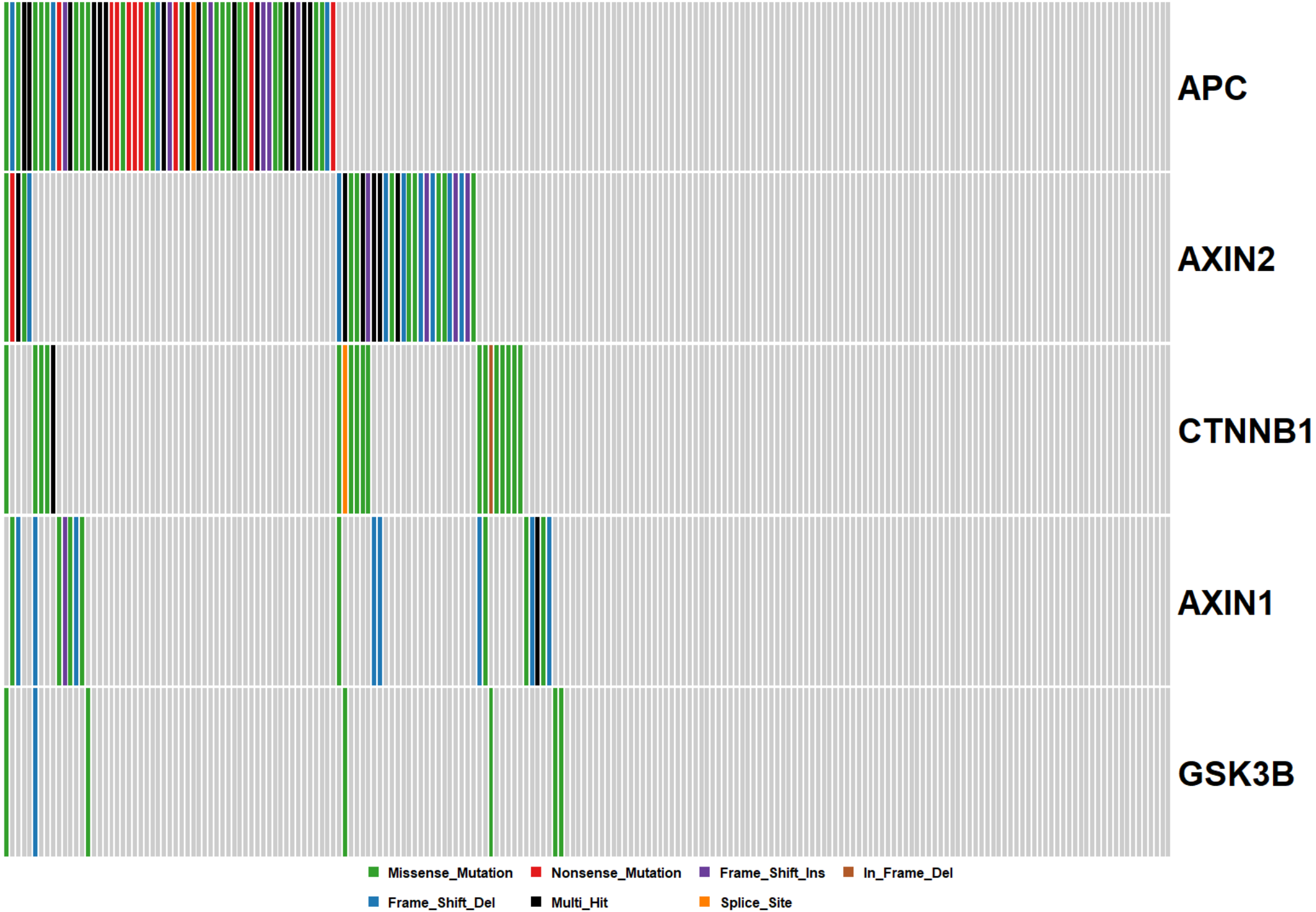
APC
AXIN2
CTNNB1
AXIN1
GSK3B
Missense_Mutation
Nonsense_Mutation
Frame_Shift_Ins
In_Frame_Del
Frame_Shift_Del
Multi_Hit
Splice_Site

All Mutations

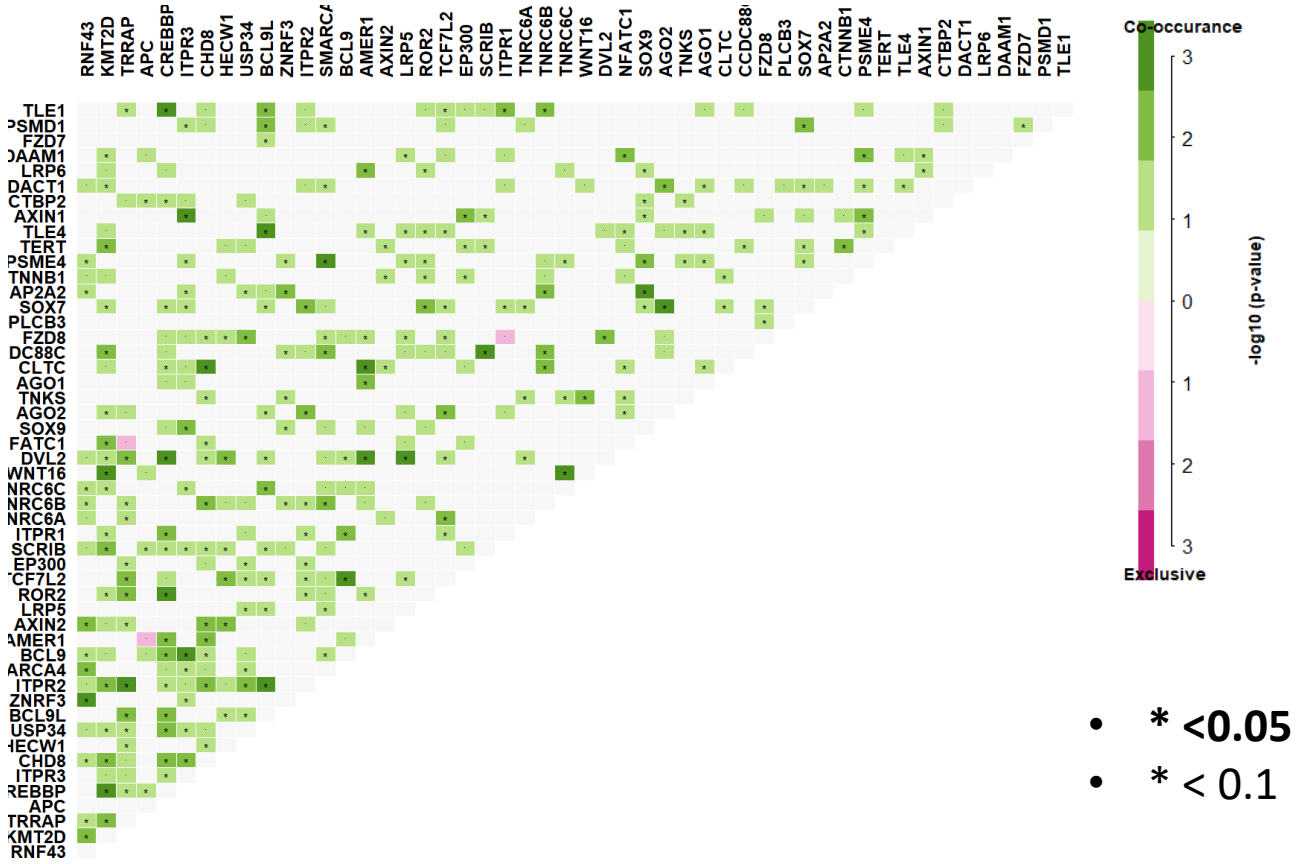

- * <0.05
- * < 0.1

Truncating Mutations

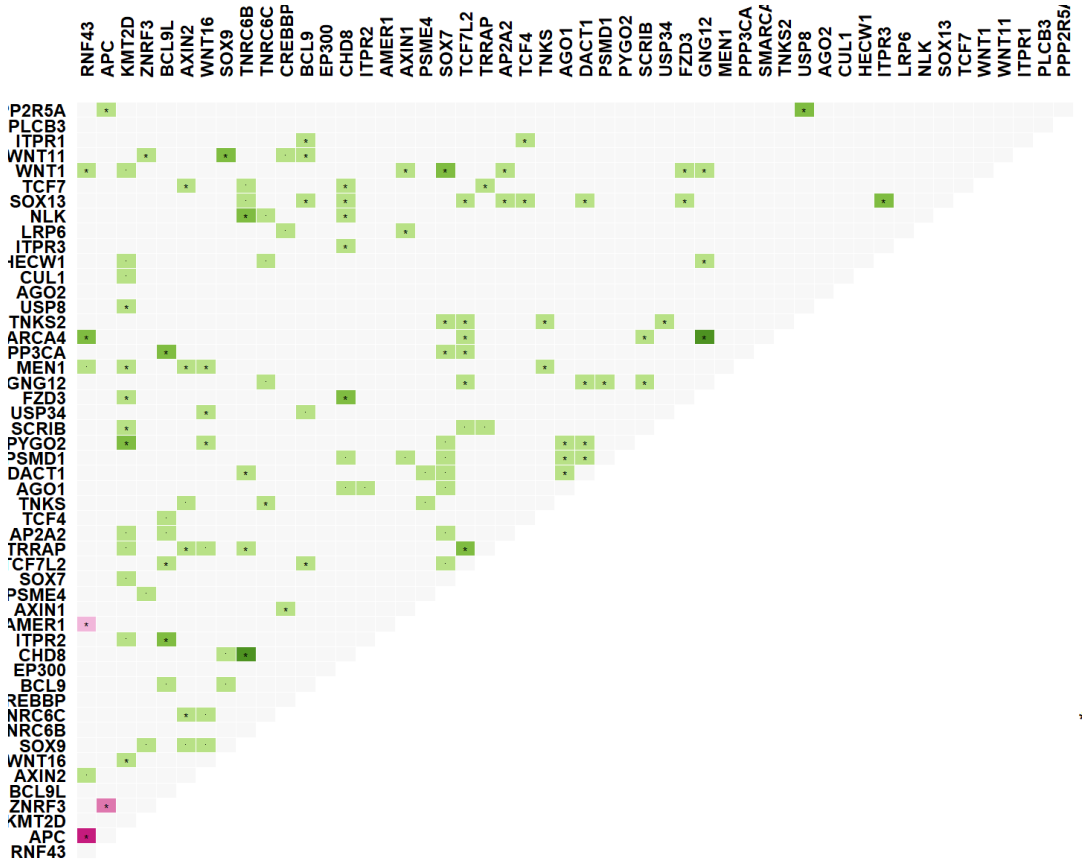

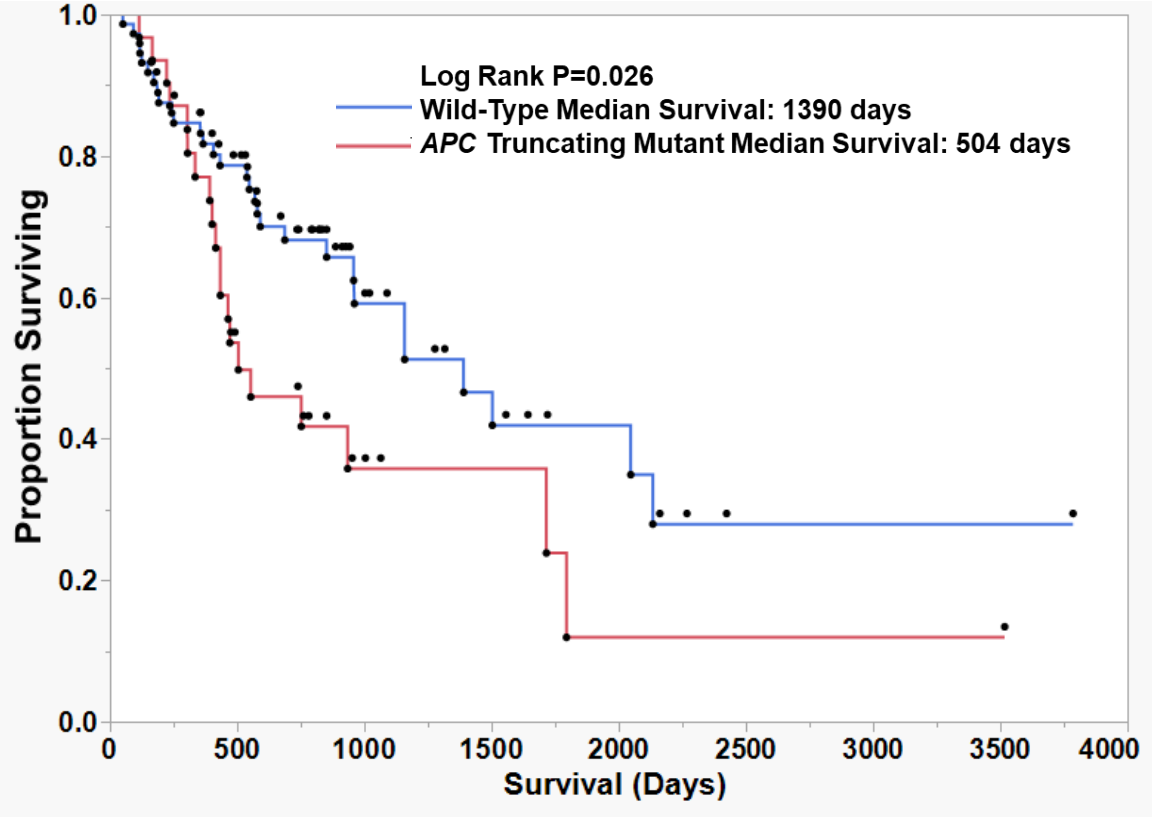
Log Rank P=0.026
Wild-Type Median Survival: 1390 days
APC Truncating Mutant Median Survival: 504 days
Proportion Surviving
1.0
0.8
0.6
0.4
0.2
0.0
0
500
1000
1500
2000
2500
3000
3500
4000
Survival (Days)

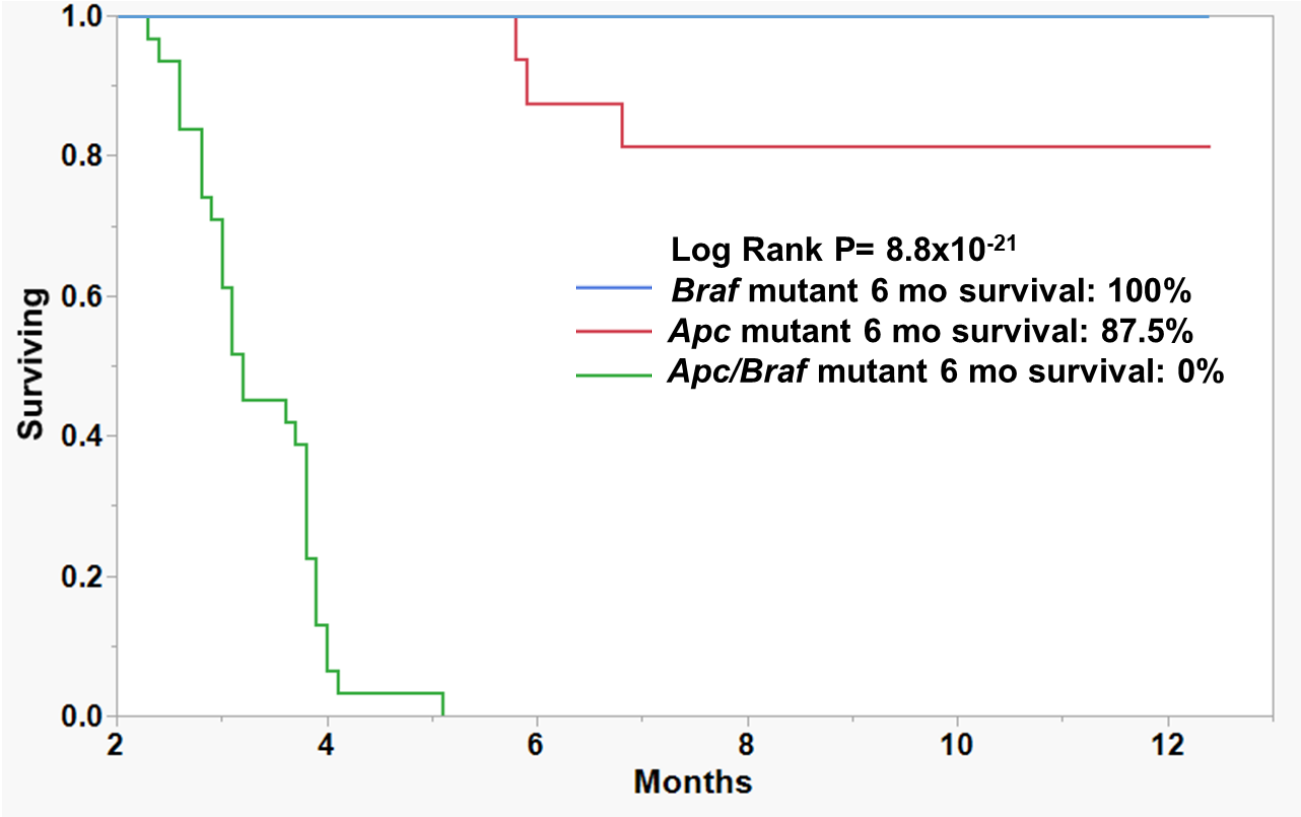
Log Rank P= 8.8x10-21
Braf mutant 6 mo survival: 100%
Apc mutant 6 mo survival: 87.5%
Apc/Braf mutant 6 mo survival: 0%
Surviving
1.0
0.8
0.6
0.4
0.2
0.0
2
4
6
8
10
12
Months

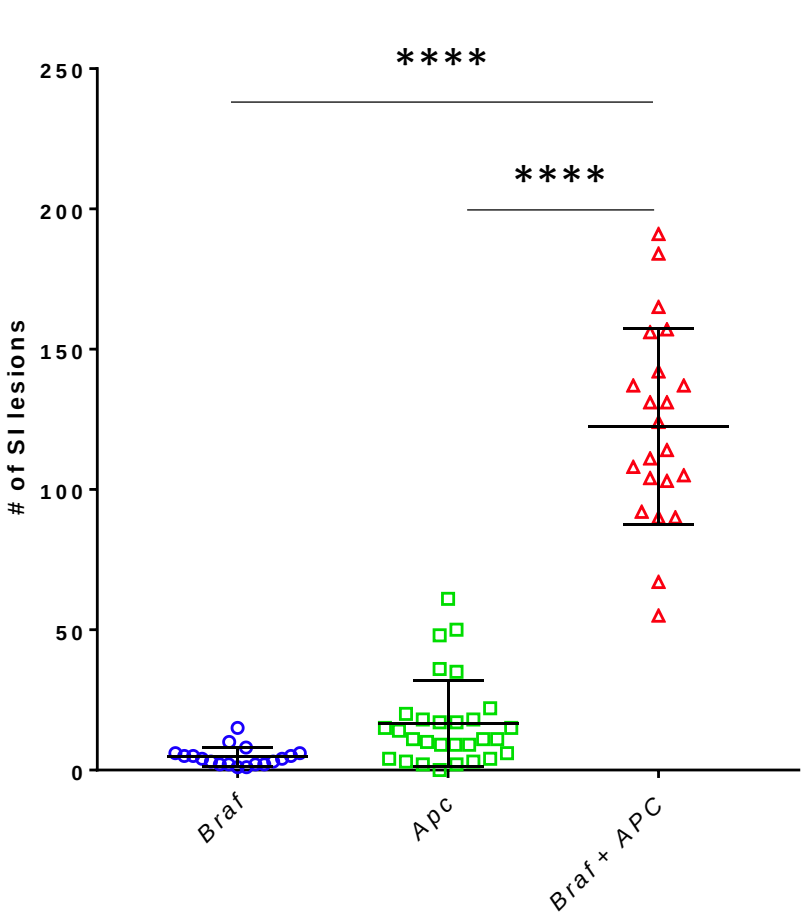
****
****
250
200
150
100
50
0
# of SI lesions
Braf
Apc
Braf + APC

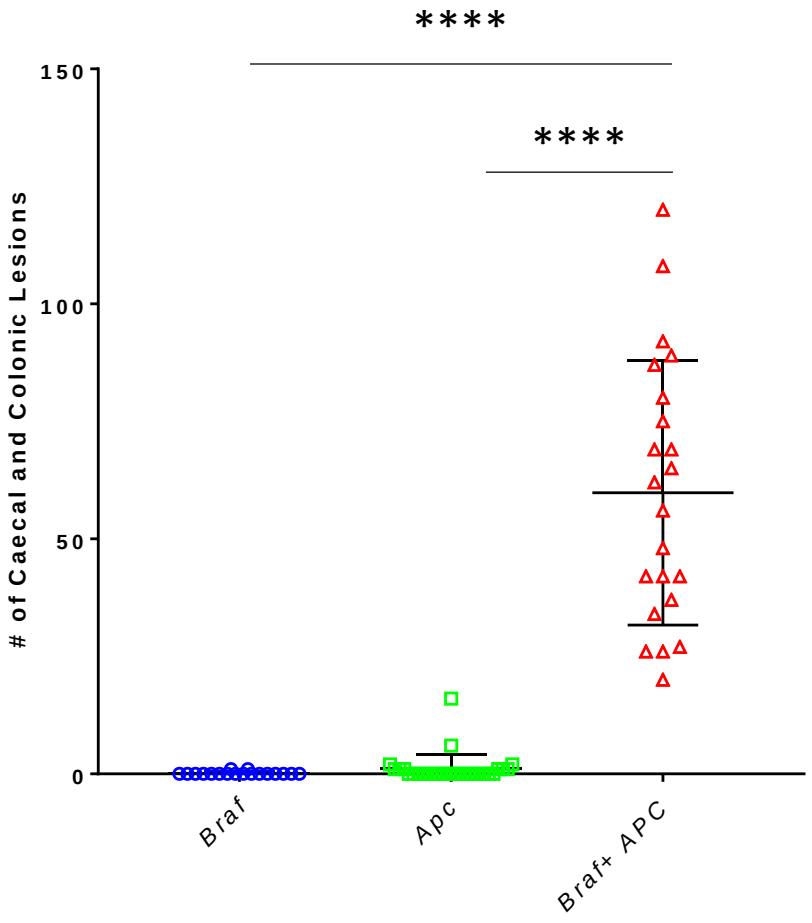
****
****
150
100
50
0
# of Caecal and Colonic Lesions
Braf
Apc
Braf+ APC

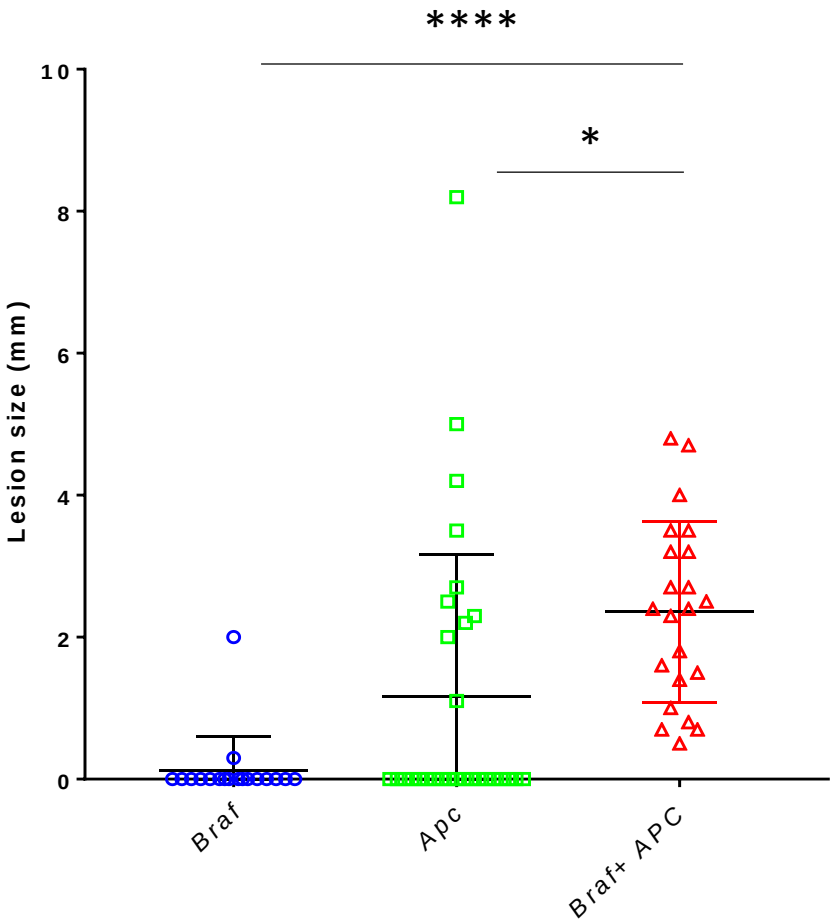
****
*
10
8
6
4
2
0
Lesion size (mm)
Braf
Apc
Braf+ APC

Figure 1: The somatic mutation landscape of WNT signaling regulators in *BRAF* mutant colorectal cancers. The 30 most frequently mutated genes in the WNT pathway are depicted. Each column corresponds to a single cancer. The colour of bars is indicative of the type of mutation with grey = wild-type. The barplot at the top of the figure represents the number of mutations in the WNT pathway a sample has. The vertical plot on the right of the figure represents the number of mutations in each gene, colour coded by mutation type.

Figure 2: Mutations in the Beta-Catenin destruction complex. Each column corresponds to a single cancer and each row a single gene.

Figure 3: Somatic interaction analysis reveals mutually exclusive mutations between gene pairs, and significant co-occurring mutations. Co-occurring mutations are indicated by green squares and mutually exclusive mutations between gene pairs in purple. The intensity of the colour is proportionate the the –log10(P-value). P-values were determined using fishers exact test.

Figure 4: Survival analysis of *BRAF* mutant human cancers by the presence or absence of truncating *APC* mutation (Left). Survival analysis of *murine* models of colorectal cancer (Right). P-values are univariate and obtained using the log-rank test.

Figure 5: Assessment of the number and size of lesions in *Apc, Braf,* and *Apc/Braf* mutant mouse models. Total lesions in the small intestine (Left), and the colon and caecum (centre). Mean size of lesions in the colon and caecum (Right)